Korea-Australia Rheology Journal
Vol. 16, No. 4, December 2004 pp. 193-199

Electrorheological characteristics of poly(o-ethoxy)aniline nanocomposite

Jun Hee Sung and Hyoung Jin Choi*
Dept. of Polymer Science and Engineering, Inha University, Incheon 402-751, Korea
(Received November 18, 2004; final revision received December 1, 2004)

Abstract

Poly(o-ethoxy)aniline (PEOA)/organoclay nanocomposite was prepared via a solvent intercalation using chloroform as a cosolvent with organically modified montmorillonite (OMMT) clay. The PEOA initially synthesized from a chemical oxidation polymerization in an acidic condition at pH = 1 was intercalated into interlayers of the clay with 25 wt% clay content. Electrical conductivity of the PEOA/OMMT nanocomposite was found to be controlled via the intercalating process. The synthesized PEOA/OMMT nanocomposite was characterized via an XRD and a TGA, and then adopted as an electrorheological (ER) material. The PEOA/OMMT synthesized with controllable electrical conductivity without a dedoping process was found to show typical ER characteristics possessing a yield stress from both steady state and dynamic measurements under an applied electric field.

Keywords : poly(o-ethoxy)aniline, nanocomposite, electrorheology, yield stress

1. Introduction

A conducting polymer/clay nanocomposite system has been introduced to improve its engineering applicability such as colloidal stability or mechanical strength (Kim *et al.*, 2002a; Kim *et al.*, 2001a) or physical properties including good thermal, environmental properties, and electrical conductivity over the pure conducting polymers, such as polypyrrole (PPy) and polyaniline (PANI) (Joo *et al.*, 2000)

As one of the novel conducting polymers, PANI contains large equilibrium phenylene ring with torsional displacements out of the plane defined by the ring bridging atoms (amine/imine nitrogens). Because of its strong inter- and intra- molecular interactions resulting in stiff backbone of the PANI, it is known to be interactable in common organic solvents. Thereby, ways to improve the solubility of PANI have been studied using some derivatives of the substituted PANIs (Mello *et al.*, 1995). Substituent groups (-CH_3, -OCH_3 or -OC_2H_5) in the monomer or polymeric chain of the PANI appear to enhance the solubility, by displaying at the same time a significant increase in electronic localization with simultaneous decrease in conductivity but an excellent solubility in a number of organic solvents. The PEOA substituted with -OC_2H_5 in PANI has been attracted to the synthetic metals community due to its good solubility and corrosion inhibition of metallic surfaces (Mello *et al.*, 1995; Macinnes, 1998). Its conductivity is lower than that of PANI within the whole doping range because of ethoxy side group which disturbs electronic conjugation of the conductivity in polymer backbone.

Meanwhile, the OMMT is a natural montmorillonite (MMT) modified with a quaternary ammonium salt of dimethyl, hydrogenatedtallow, 2-ethylhexyl quaternary ammonium. As the most affluent natural clay, the MMT consists of a sheet of octahedral alumina between two tetrahedrally coordinated silica sheets. Originally, the clay consists of anionically charged layers of aluminum/magnesium silicates and small cations such as sodium or potassium located in silicate interlayer galleries (Ogawa and Takizawa, 1999; Wu and Lerner, 1993). Since the substituted ions for higher charge in the octahedral (e.g., Mg^{2+} replacing Al^{3+}) and tetrahedral (e.g., Al^{3+} replacing Si^{4+}) sheets show negatively charged layers, these silicate layers can be exchanged with organic cationic molecules and then swelled under a polar solvent.

Intercalation of polymer in layered hosts has been introduced to synthesize nanophase organic-inorganic hybrids of polymer/clay nanocomposites, and it is well known that they usually exhibit superior physical and mechanical properties, such as solvent resistance, ionic conductivity, optical properties, heat resistance, tensile modulus and strength, decreased gas permeability and flammability when compared with the pristine commercial polymers or conventional polymer composites (Galgali and Ramesh, 2001; Usuki *et al.*, 1993; Messermith and Giannelis, 1995; Choi *et al.*, 2001b; Gilman, 1999; Okada *et al.*, 2003; Ryu *et al.*, 2004; Sur *et al.*, 2003). The inorganically constrained environment at internal gallery of the clay gives a significant effect on polymer structure, properties, and

*Corresponding author: hjchoi@inha.ac.kr

electrical conduction mechanism. Conducting polymer/clay nanocomposite system has been thus introduced to improve the applicabilities or physical properties of the conducting polymers. This enhances not only better processability (Kim *et al.*, 2002a; Kim *et al.*, 2001a) but also characteristics. The fabrication of nanocomposite materials shows the high potential for advanced electrochromic devices (Roth and Graupner, 1993), electromagnetic (Wessling, 1998), mechanical, thermal (Lan *et al.*, 1994), and chemical sensing applications (Shim *et al.*, 1991).

Nanocomposites of conducting polymers and inorganic materials have been also used for electrorheological (ER) fluids (Kim *et al.*, 2001b; Park *et al.*, 2001), which are composed of a suspension of micro-sized semiconducting or conducting particles in an insulating fluid. The applied electric field induces chainlike structures of particles in surrounding fluid, thus changing from liquid-like to solid-like phase due to the interaction among the particles, which can be polarized in the order of milliseconds. ER fluids have potential applications such as torque transducers, and vibration attenuators such as shock absorbers, because of a rapid and reversible change of viscosity with an applied electric field (Park and Park, 2001; Kim *et al.*, 1999).

Most ER fluids are made of particulate materials (Kim *et al.*, 2001c), including inorganic non-metallic, organic, and polymeric semi-conducting materials, dispersed into an insulating non-polar liquid. Various polymeric particles have been used as ER materials including many conducting polymers, such as, PANI (Lee *et al.*, 1998), PPy (Goodwin *et al.*, 1997), poly(p-phenylene) (Plocharski *et al.*, 1997) and PANIs derivatives, *e.g.*, PANI nanoparticles (Cho *et al.*, 2004b), microencapsulated PANI (Lee *et al.*, 2001), PANI core-shell structure (Cho *et al.*, 2002), and PANI nanocomposites with clay (Kim *et al.*, 2001b) or MCM-41 (Cho *et al.*, 2004a) which are thermally stable and relatively easy to synthesize. These typical conducting polymers and modified particles are based on a π-conjugated electron system in the polymer backbone.

In this study, we synthesized soluble PEOA and then prepared nanocomposite with PEOA (25 wt%) and OMMT via a solvent intercalation method using chloroform ($CHCl_3$). We examined the characteristics of PEOA/OMMT nanocomposite by correlating the intercalated nanostructures with electrical and thermal properties. Based on the electrical conductivity which can be easily controlled by the PEOA intercalation into clay gallery, we investigated ER response of the PEOA/OMMT nanocomposite based suspensions.

2. Experimental

Polymer solution intercalation is based on a solvent system in which the polymer is soluble and the silicate layers are swellable (Greenland, 1963). The silicate layer is swollen in a solvent and then polymer chains are intercalated by displacing the solvent. The driving force for polymer intercalation into layered silicate from solution is the entropy gained by desorption of solvent molecules, which compensates for the entropy decrease of the confined, intercalated chains (Then, 1979). As a soluble conducting polymer in organic solvents, the PEOA particle was synthesized initially following our previously reported method (Sung *et al.*, 2003). A 0.6 mole ethoxyaniline monomer (Aldrich, USA) in 400 ml of 1 M HCl was stirred for 2 h, and the polymerization was initiated by a solution of 0.36 mole ammonium persulfate in 240 ml of 1 M HCl. The reaction was performed at 25°C. After polymerization of the PEOA particles, final products were dried at room temperature for 2 days using a vacuum oven. Because the PEOA particles were polymerized in acidic condition (pH = 1) which was measured in reaction product slurry, the particles showed a doped state in the polymer backbone. The Cloisite 25A (Southern Clay Product, USA) (OMMT) was used as the organic clay. The OMMT in chloroform was swollen for 1 day. The PEOA particle was also dissolved in chloroform, concurrently. Both clay and PEOA in chloroform solutions were mixed together at same concentration (0.5 wt%) for each component, and stirred for 1 day. The mixed solution was filtered and dried at room temperature for 2 days using a vacuum oven. The nanocomposite obtained as powder form of products was with 25% weight content of PEOA in the PEOA/OMMT composite.

The shape and size of the final products were observed using a scanning electron microscopy (SEM, S-4300, Hitachi). The image by the intercalation of PEOA/OMMT nanocomposite was observed using a transmission electron microscope (TEM) (CM 200, Philips). The XRD measurement was performed using the Rigaku DMAX 2500 (λ = 1.54 Å) diffractometer. The thermal properties were also examined using a thermogravimetric analyzer (TGA, TA instrument Q50, USA). The electrical conductivity of PEOA particle and nanocomposite was measured using a 2-probe method with a pressed disk of polymer with silver electrodes on each side. The pellet of PEOA particle was prepared using a 13 mm KBr pellet die, and the pellet resistance was measured using a picoammeter (Keithley model 487, Cleveland, U.S.A) with a conductivity cell. The conductivity (σ) (S/cm) was then obtained from $\sigma = d/(A \cdot R)$. Here d is the thickness (cm), A is the surface area (cm^2) and R is the resistance of the pellet ($1/S$).

In addition, the ER properties were measured using a commercially available rotational rheometer (Physica MC 120, Stuttgart) with a Couette geometry (Z3-DIN) equipped with a high-voltage generator (Meyport series 230). Several DC electric field strengths (0~3.0 kV/mm) were applied to the bob. The maximum stress is 1,141 Pa and capacity of ER fluid for measuring has about 17 ml in the

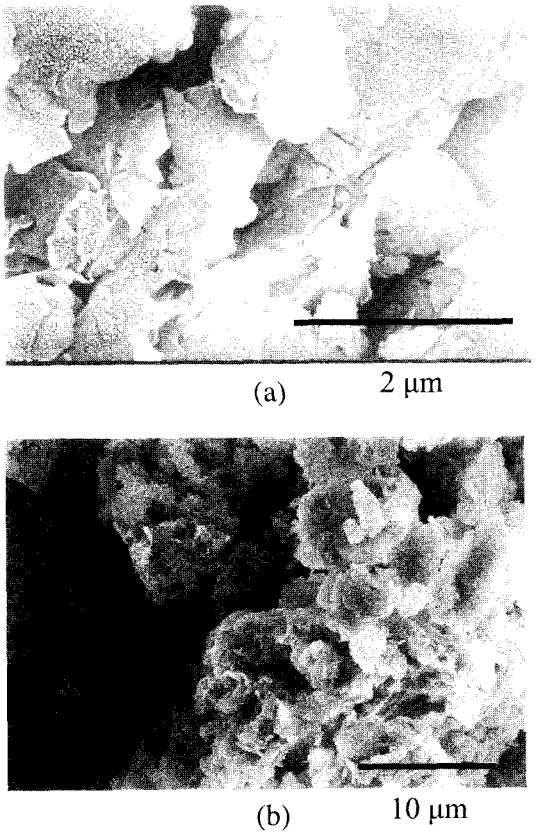

Fig. 1. SEM images of the (a) OMMT and (b) PEOA/OMMT nanocomposite.

1.06 mm of the gap. Temperature can be changed from –40 to 150°C by circulating oil bath (VISCOTHERM VT 100).

3. Results and Discussion

The SEM photographs of (a) pristine OMMT and (b) PEOA/OMMT nanocomposite are presented in Fig. 1. While the PEOA particle showed aggregation of round-shaped small particles, the OMMT image displayed sheet-like plates. Thereby, the PEOA/OMMT nanocomposite possesses two characteristic morphologies of round-shape of the particles and plate-like OMMT, since the dissolved PEOA could combine with surface of OMMT and intercalate into OMMT, anticipating the nanoscopic intercalation of PEOA chain with OMMT interlayers. Fig. 2 displays the sectional micrograph using microtomed nanocomposites by TEM. The image of PEOA/OMMT nanocomposites confirms successful intercalation into OMMT. The soluble PEOA particles were well dispersed in the interlayer of OMMT.

The Bragg's law is expressed by,

$$n\lambda = 2d \sin \theta \quad (1)$$

where λ the X-ray wavelength (0.154 nm), d the spacing between the atomic planes, and θ the angle between the X-ray beam and the atomic plane. Constructive interference occurs for integer values of n. By measuring θ for a known wavelength the Bragg spacing d can be determined. Fig. 3 shows the XRD patterns for PEOA particle before intercalation and PEOA/OMMT nanocomposite. The peak at $2\theta = 4.8^{\circ}$ (d-spacing: 1.84 nm) corresponds to crystallographic planes of the pristine OMMT clay layer, (001) basal spacing reflection. The d-spacing expansion was identified from the shift of the diffraction peak to lower angles of $2\theta = 4.18^{\circ}$ (d-spacing: 2.11 nm) of PEOA/OMMT (Scaife, 1989; Cho *et al.*, 2003). Table 1 presents the d-spacing expansion and the electrical conductivity of PEOA/OMMT nanocomposite. Electrical conductivity of pure PEOA obtained by 2-probe method was 2.0×10^{-4} S/cm. This effect of particle conductivity was an important factor for the delocalization of charge carriers. The changes

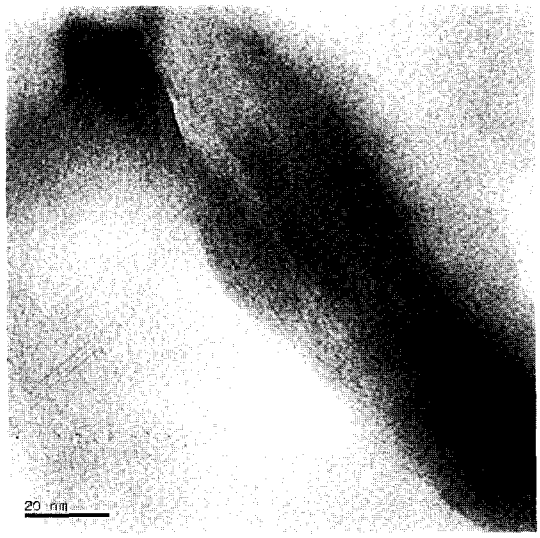

Fig. 2. TEM photograph of the PEOA/OMMT nanocomposite.

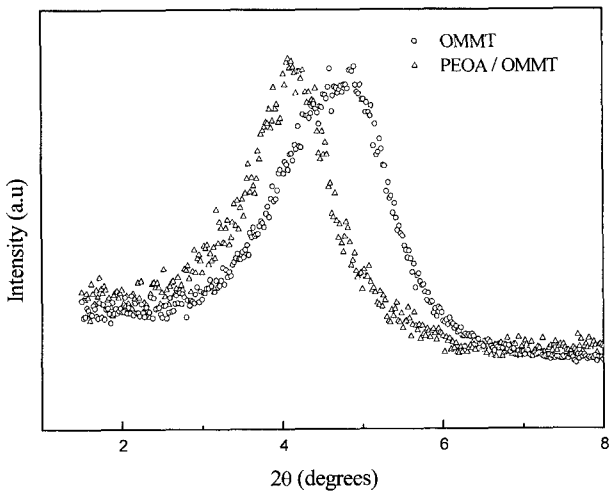

Fig. 3. XRD of the PEOA, OMMT, and PEOA/OMMT nanocomposite.

Table 1. XRD data and electrical conductivity of PEOA and PEOA/OMMT nanocomposite

	d-spacing (nm)	2θ (°)	Conductivity (S/cm)
PEOA			2.0×10^{-4}
OMMT	1.84	4.80	-
PEOA/OMMT	2.11	4.18	7.3×10^{-10}

of electrical conductivity was attributed to the fact that intercalation into clay takes a role of resistance of the PEOA (Conrad *et al.*, 1999). The electrical conductivity of PEOA/OMMT nanocomposite was found to become lower than that of pure PEOA. It has been reported that the electrical conductivity of composites decreases in the presence of insulating organoclay since the clay layers interrupt the delocalization of charge carriers and weaken the interchain interaction and induce more disorder state, resulting in lower electrical conductivity (Kim *et al.*, 2001a). This nanocomposite with such a low electrical conductivity can be directly used as ER materials (Choi *et al.*, 2001a). As expected by both XRD and TEM analyses, these results are attributed to the internal structure of nanocomposites. It can, therefore, be conjectured that PEOA chains in the interlayer spaces are more extended than in the bulk form and charge carriers can move more freely (Kim *et al.*, 2002b; Jia *et al.*, 2002).

Fig. 4 shows the TGA thermograms of weight loss as a function of temperature for PEOA and its nanocomposite with PEOA. The onset decomposition temperature of nanocomposite is higher than that of PEOA. This behavior confirms the increased thermal stability of nanocomposite. Also, the residual weight of nanocomposite is much higher than that of PEOA, showing that the thermal stability of nanocomposites increases due to the retardation effect of organoclay platelets on the decomposition of the polymer.

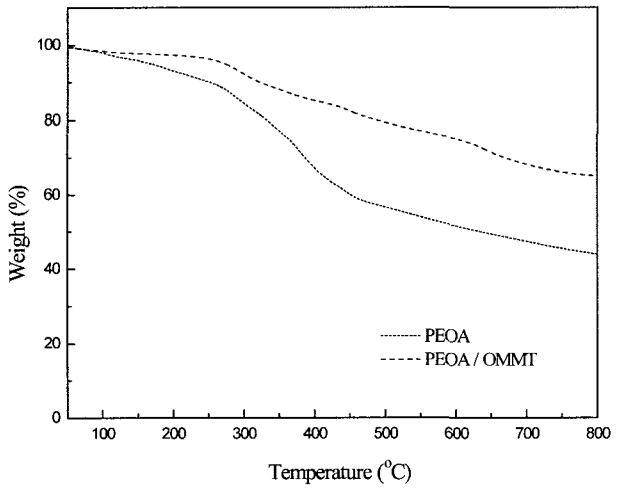

Fig. 4. TGA curves of PEOA and PEOA/OMMT nanocomposite.

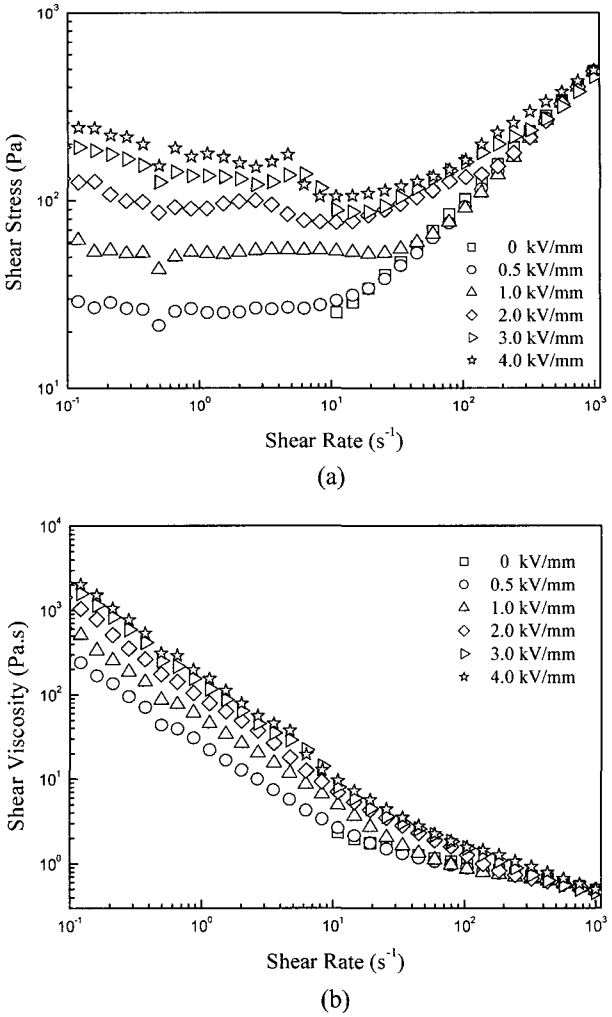

Fig. 5. (a) Shear stress and (b) shear viscosity *vs.* shear rate for 20 wt% PEOA/OMMT nanocomposite based ER fluid.

The PEOA/OMMT nanocomposite based ER fluid with 20 wt% of particle was prepared. The ER property of the PEOA/OMMT nanocomposite suspension upon application of an electric field displays a Bingham fluid behavior. Fig. 5(a) and (b) present the dependence of shear stress and shear viscosity as a function of electric field strength for PEOA/OMMT nanocomposite dispersed in silicone oil. The electrostatic force of inter-particle shows at low shear rate region and the hydrodynamic force of each particle presents at high shear rate region. The plateau region describes the overcoming of electrostatic force over external shear force. That is, the relaxation time is faster in case of low electric field strength. However, at the higher electric field, the shear stress shows the high values. The non-Newtonian shear thinning behavior is also shown in Fig. 5 (b). When an electric field was applied to this suspension, the shear stress abruptly increased over the entire shear rate range, and yield stresses appeared as in a Bingham fluid.

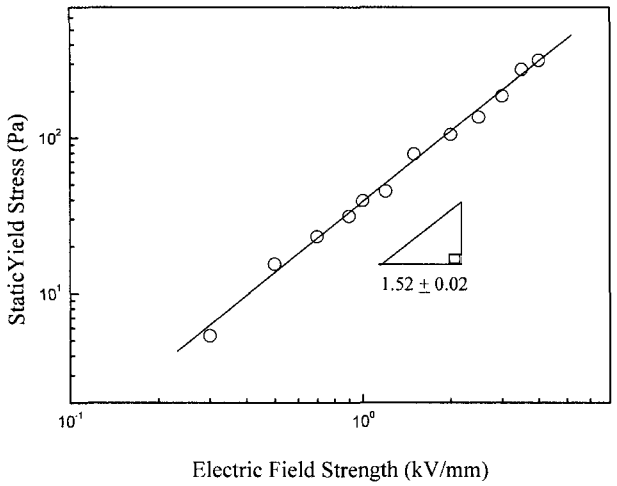

Fig. 6. Static yield stress *vs.* electric field strengths of 20 wt% PEOA/OMMT nanocomposite based ER fluid.

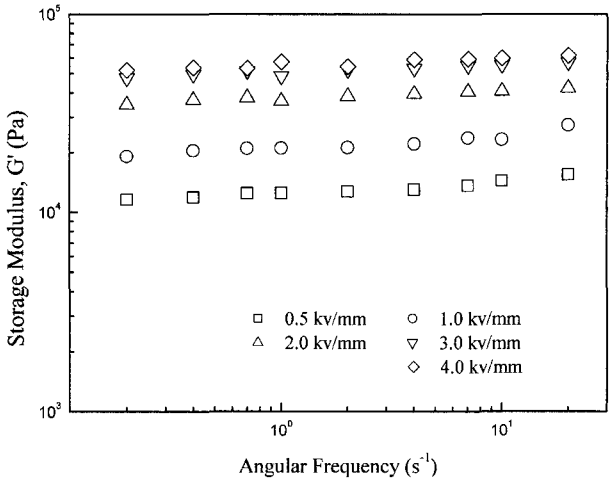

Fig. 7. G' as a function of angular frequency for 20 wt% PEOA/OMMT nanocomposite based ER fluid.

Fig. 6 presents the dependence of static yield stress on electric field strength of PEOA/OMMT based ER fluid. The ER fluid was stressed by an applied mechanical torque until the fibrillar chain structure of the suspended particles was broken to lead flow, and the stress at starting point of flow is termed as a static yield stress. The slope displays approximately 1.52 slightly deviating from the exponent 1.5 of the conductivity model due to irregular shape and size of the dispersed particle. In particular, OMMT possessing a high aspect ratio is related with the ER effect with flow direction.

The yield stress originates from the attractive forces between particles, by fully taking into account both polarization and conduction models. The nonlinear conductivity effect with the bulk conducting particle model and the exponent of the power law is 1.5 at high electric field strengths. The previously proposed universal yield stress equation which can fit both polarization and conduction models at the same time is as follows (Choi *et al.*, 2001):

$$\tau_y(E_o) = \kappa E_o^2\left(\frac{\tanh\sqrt{E_o/E_c}}{\sqrt{E_o/E_c}}\right) \tag{2}$$

where κ depends on the dielectric constant and the particle volume fraction, and E_c is the critical electric field strength, which is proportional to the particle conductivity. We also found that E_c is influenced by the conductivity mismatch between the particle and medium liquid and is weakly dependent on the volume fraction and for higher electric field case, Eq. (2) becomes as follows giving the exponent of 1.5 as a function of an applied electric field,

$$\tau_y(E_o) = \kappa E_o^2(\sqrt{E_o/E_c})^{-1} = \kappa\sqrt{E_c}E_o^{3/2} \propto E_o^{3/2}$$

$$\text{since } \tanh\sqrt{E_o/E_c} \cong 1 \text{ for } E_o \gg E_c. \tag{3}$$

Fig. 7 shows the G' remained constant of PEOA/OMMT based ER fluid 20 wt% of particles as a function of angular frequency at different electric field strengths. The linear region viscoelastic region shows at overall region and the higher G' with induced high electric field strength. A small strain (0.002) as a linear viscoelastic region was applied and the frequency was fixed at 10 Hz. The inter-particle interactions due to polarization contribute to the enhancement of the dynamic moduli and the steady shear viscosity to a great extent. The polarization forces between the particles increase with increasing the electric field strength resulting from increasing the particle chain length and magnitude of G'.

4. Conclusions

The soluble conducting PEOA was prepared by the chemical oxidation polymerization and PEOA/OMMT nanocomposite was intercalated via a solvent casting process. The degree of d-spacing of PEOA/OMMT nanocomposites was expanded to 2.11 nm compared to the pristine clay (1.84 nm). The electrical conductivity of PEOA/OMMT could be controlled by intercalation into clay, and was much lowered than that of PEOA. Thereby, it is found that the synthesis of PEOA/OMMT is one of the best ways to prepare ER sample without dedoping the conducting polymer. We found that the clay layers interrupt the delocalization of charge carriers and weaken the interchain intercalation and induce more disorder, resulting in lower electrical conductivity. The ER fluid showed the Bingham fluid behavior possessing yield stress and displayed a linear viscoelastic response at given angular frequency range.

Acknowledgement

This study was supported by research grants from the Korea Science and Engineering Foundation (KOSEF)

through the Applied Rheology Center (ARC), an official KOSEF-created engineering research center (ERC) at Korea University, Seoul, Korea.

References

Cho, M.S., H.J. Choi and W.S. Ahn, 2004a, Enhanced electrorheology of coating polyaniline confined in MCM-41 channels, *Langmuir* **20**, 202-207.

Cho, M.S., S.Y. Park, J.Y. Whang and H.J. Choi, 2004b, Synthesis and electrical properties of polymer composites with polyaniline nanoparticles, *Mater. Sci. Eng. C* **24**, 15-18.

Cho, M.S., Y.H. Cho, H.J. Choi and M.S. Jhon, 2003, Synthesis and electorheological characteristic of polyaniline-coated poly (methylmethacrylate) microsphere: size effect, *Langmuir* **19**, 5875-5881.

Cho, Y.H., H.J. Choi, M.S. Cho and M.S. Jhon, 2002, Electrorheological characterization of polyanilinecoated poly(methyl methacylate) suspensions, *Colloid Polym. Sci.* **280**, 1062-1066.

Choi, H.J., M.S. Cho, J.W. Kim, C.A. Kim and M.S. Jhon, 2001, A yield stress scaling function for electrorheological fluids, *Appl. Phys. Lett.* **78**, 3806-3808.

Choi, H.J., J.W. Kim, J. Joo and B.H. Kim, 2001a, Synthetic and electrorheology of emulsion intercalated PANI-clay nanocomposite, *Synth. Met.* **121**, 1325-1326.

Choi, H.J., S.G. Kim, Y.H. Hyun and M.S. Jhon, 2001b, Preparation and rheological characteristics of solvent-cast poly(ethylene oxide)/montmorillonite nanocomposites, *Macromol. Rapid Commun.* **22**, 320-325.

Conrad, H., C. Wu and X. Tang, 1999, Conductivity in electrorheology, *Int. J. Mod. Phys. B* **13**, 1729-1738.

Galgali, G., C. Ramesh and A. Lele, 2001, A rheological study on the kinetics of hybrid formation in polypropylene nanocomposites, *Macromolecules* **34**, 852-858.

Gilman, J.W., 1999, Flammability and thermal stability studies of polymer layered-silicate (clay) nanocomposites, *Appl. Clay Sci.* **15**, 31-49.

Goodwin, J.W., G.M. Markham and B. Vincent, 1997, Studies on model electrorheological fluids, *J. Phys. Chem. B* **101**, 1961-1967.

Greenland, D.J., 1963, Adsorption of poly(vinyl alcohols) by montmorillonite, *J. Colloid Sci.* **18**, 647-664.

Jia, W., E. Segal, D. Kornemandel, Y. Lamhot, M. Narkis and A. Siegmann, 2002, Polyamide-DBSA/organophillic clay nanocomposite; synthesis and characterization, *Synth. Met.* **128**, 115-120.

Joo, J., J.K. Lee, S.Y. Lee, K.S. Jang, E.J. Oh and A.J. Epstein, 2000, Physical characterization of electrochemically and chemically synthesized polypyrroles, *Macromolecules* **33**, 5131-5136.

Kim, B.H., J.H. Jung, J.W. Kim, H.J. Choi and J. Joo, 2001a, Effect of dopant and clay on nanocomposites of polyaniline (PAN) intercalated into Na^+-montmorillonite (Na^+-MMT), *Synth. Met.* **121**, 1311-1312.

Kim, B.H., J.H. Jung, J. Joo, A.J. Epstein, K. Mizoguchi, J.W. Kim and H.J. Choi, 2002a, Nanocomposite of polyaniline and Na^+-montmorillonite clay, *Macromolecules* **35**, 1419-1423.

Kim, D.H., S.H. Chu, K.H. Ahn and S.J. Lee, 1999, Dynamic simulation of squeezing flow of ER fluids using parallel processing, *Korea-Australia Rheol. J.* **11**, 233-240.

Kim, J.W., S.G. Kim, H.J. Choi, M.S. Suh, M.J. Shin and M.S. Jhon, 2001b, Synthesis and eectrorheological characterization of polyaniline and Na^+-montmorillonite clay nanocomposite, *Int. J. Mod. Phys. B* **15**, 657-664.

Kim, S.G., H.J. Choi and M.S. Jhon, 2001c, Preparation and characterization of phosphate cellulose-based electrorheological fluids, *Macromol. Chem. Phys.* **202**, 521-526.

Kim, T.H., L.W. Jang, D.C. Lee, H.J. Choi and M.S. Jhon, 2002b, Synthesis and rheology of intercalated polystyrene/Na^+-montmorillonite nanocomposite, *Macromol. Rapid Commun.* **23**, 191-195.

Lan, T., P.D. Kaviratna and T.J. Pinnavaia, 1994, On the natural of polyimide-clay hybrid composites, *Chem. Mater.* **6**, 573-575.

Lee, D.K., S.H. Lee, K. Char and J. Kim, 2000, Expansion distribution of basal spacing of the silicate layers in polyaniline/Na-montmorillonite nanocomposites monitored with X-ray diffraction, *Macromol. Rapid Commun.* **21**, 1136-1139.

Lee, H.J., B.D. Chin, S.M. Yang and O.O. Park, 1998, Surfactant effect on the stability and electrorheological properties of polyaniline particle suspension *J. Colloid Interf. Sci.* **206**, 424-438.

Lee, Y.H., C.A. Kim, W.H. Jang, H.J. Choi and M.S. Jhon, 2001, Synthesis and electrorheological characteristics of microencapsulated polyaniline particles with melamine-formaldehyde resins, *Polymer* **42**, 8277-8283.

Lu, Y., G. Shi, C. Li and Y. Liang, 1998, Thin polypyrrole films prepared by chemical oxidative polymerization, *J. Appl. Polym. Sci.* **70**, 2169-2172.

Macinnes, D. and B.L. Funt, 1998, Poly-o-methoxyaniline: A new soluble conducting polymer, *Synth. Met.* **25**, 235-242.

Mello, S.V., L.H.C. Mattoso, R.M. Faria and O.N. Oliveira, 1995, Effect of doping on the fabrication of Langmuir and Langmuir-Blodgett films of poly(o-ethoxyaniline), *Synth. Met.* **71**, 2039-2040.

Messermith, P.B. and E.P. Giannelis, 1995, Synthesis and barrier properties of poly(ε-caprolactone)-layered silicate nanocomposites, *J. Polym. Sci. Part A: Polym. Chem.* **33**, 1047-1057.

Ogawa, M. and Y. Takizawa, 1999, Intercalation of alkylammonium cations into a layered titanate in the presence of macrocylic compounds, *Chem. Mater.* **11**, 30-32.

Okada, K., T. Mitsunaga and Y. Nagase, 2003, Properties and particles dispersion of biodegradable resin/clay nanocomposites, *Korea-Australia Rheol. J.* **15**, 43-50.

Park, J.H. and O.O. Park, 2001, Electrorheology and magnetorheology, *Korea-Australia Rheol. J.* **13**, 13-17.

Park, J.H., Y.T. Lim and O.O. Park, 2001, New approach to enhance the yield stress of electrorheological fluids by polyaniline-coated layered silicate nanocomposites, *Macromol. Rapid Commun.* **22**, 616-619.

Plocharski, J., H. Drabik, H. Wycislik and T. Ciach, 1997, Electrorheological properties of polyphenylene suspensions, *Synth. Met.* **88**, 139-145.

Roth, S. and W. Graupner, 1993, Conductive polymers: evaluation of industrial applications, *Synth. Met.* **57**, 3623-3631.

Ryu, J.G., S.W. Park, H. Kim and J.W. Lee, 2004, Power ultra-

sound effects for in situ compatibilization of polymer-clay nanocomposites, *Mater. Sci. Eng. C* **24**, 285-288.

Scaife, B.K.P. 1989, In: Principles of dielectrics, Clarendon Press, Oxford, 66.

Shim, Y.-B., D.E. Stilwell and S.-M. Park, 1991, Electrochemistry of conductive. X: polyaniline-based potentionmetric sensor for dissolved oxygen, *Electroanalysis* **3**, 31-36.

Sung, J.H., J.W. Kim, H.J. Choi and S.B. Choi, 2003, Synthesis and characterization of organoclay nanocomposite with poly(o-ethoxyaniline), *Synth. Met.* **135-136**, 19-20.

Sur, G.S., S.G. Lyu and J.H. Chang, 2003, Synthesis and LCST behavior of thermosensitive poly(N-isopropylacryamide-clay nanocomposites, *J. Ind. Eng. Chem.* **9**, 58-62.

Then, B.K.G. 1979, Formation and properties of clay-polymer complexes, New York: Elsevier.

Usuki, A., M. Kawasumi, Y. Kojima, A. Okada, T. Kurauchi and O. Kamigaito, 1993, Swelling behavior of montmorillonite cation exchanged for w-amino acids by e-caprolactam. *J. Mater. Res.* **8**, 1174-1178.

Wessling, B., 1998, Dispersion as the link between basic research and commercial applications of conductive polymers (polyaniline), *Synth. Met.* **93**, 143-154.

Wu, J. and M. Lerner, 1993, Structural, thermal, and electrical characterization of layered nanocomposites derived from sodium-montmorillonite and polyethers, *Chem. Mater.* **5**, 835-838.